

Molecular Insight into Different Denaturing Efficiency of Urea, Guanidinium, and Methanol: A Comparative Simulation Study

Takahiro Koishi,*[†] Kenji Yasuoka,[‡] Soohaeng Yoo Willow,[§] Shigenori Fujikawa,^{||} and Xiao Cheng Zeng*,[†]

[†]Department of Applied Physics, University of Fukui, 3-9-1 Bunkyo, Fukui 910-8507, Japan

[‡]Department of Mechanical Engineering, Keio University, Yokohama 223-8522, Japan

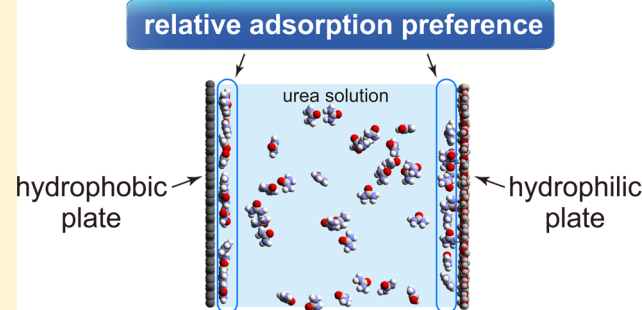
[§]Department of Chemistry, Pohang University of Science and Technology, San 31, Hyojadong, Namgu, Pohang 790-784, South Korea

^{||}International Institute for Carbon-Neutral Energy Research (WPI-I2CNER), Kyushu University, 744 Motooka, Nishi-ku, Fukuoka 819-0395, Japan

[†]Department of Chemistry, University of Nebraska, Lincoln, Nebraska 68588, United States

Supporting Information

ABSTRACT: We have designed various nanoslit systems, whose opposing surfaces can be either hydrophobic, hydrophilic, or simply a water-vapor interface, for the molecular dynamics simulation of confined water with three different protein denaturants, i.e., urea, guanidinium chloride (GdmCl), and methanol, respectively. Particular attention is placed on the preferential adsorption of the denaturant molecules onto the opposing surfaces and associated resident time in the vicinal layer next to the surfaces, as well as their implication in the denaturing efficiency of different denaturant molecules. Our simulation results show that among the three denaturants, the occupancy of methanol in the vicinal layer is the highest while the residence time of Gdm is the longest. Although the occupancy and the residence time of urea in the vicinal layer is less than those of the other two denaturant molecules, urea entails “all-around” properties for being a highly effective denaturant. The distinct characteristics of three denaturants may suggest a different molecular mechanism for the protein denaturation. This comparative simulation by design allows us to gain additional insights, on the molecular level, into the denaturation effect and related hydrophobic effect.



1. INTRODUCTION

Urea, guanidinium (Gdm), and methanol all have the capability to denature proteins. Among the three, urea and Gdm are widely used as strong denaturants although mechanisms of the denaturation are still incompletely understood. A common structural feature of these denaturant molecules is the existent of both hydrophilic atomic sites and a hydrophobic section or group. For example, urea possesses a carbonyl and two amine groups which favor hydrophilic interaction, while its flat structure favors hydrophobic interaction. To differentiate the role of these functional groups in denaturation, a systematic and comparative study is required.

To date, many molecular simulation studies of aqueous urea solutions^{1–4} with proteins or oligomers have been reported in order to understand the mechanism of protein denaturation at the molecular level.^{5–17} In addition, molecular simulations of Gdm ions in water^{18–25} have also been performed. Two distinctively different mechanisms have been proposed to explain the effect of denaturation, namely, the “indirect mechanism”^{16,18} in which denaturant disrupts the structure of

water in the hydration shell of proteins or the “direct mechanism”^{4–14,19} in which the denaturant interacts directly with a protein through the electrostatic and van der Waals (vdW) interactions. A few previous studies also suggest that both direct and indirect mechanisms may be involved in urea-induced chemical denaturation.^{2,15} Nevertheless, a majority of researchers support the direct mechanism.

For the direct mechanism in which urea interacts directly with the protein, two dominant interactions are proposed: the electrostatic interaction^{5–8,19} and the vdW interaction.^{4,10–14} In the electrostatic interaction model, urea interacts directly with the charged side chain and protein backbone via hydrogen-bonding interaction.^{5–8} For example, O’Brien et al.¹⁹ indicated that, in urea or guanidinium chloride (GdmCl) solutions, proteins can unfold due to hydrogen bonding of denaturants to charged side chains and backbone carbonyl groups. To support the vdW interaction model, Hua et al.¹¹ pointed out the important role

Received: December 13, 2012

Published: April 17, 2013



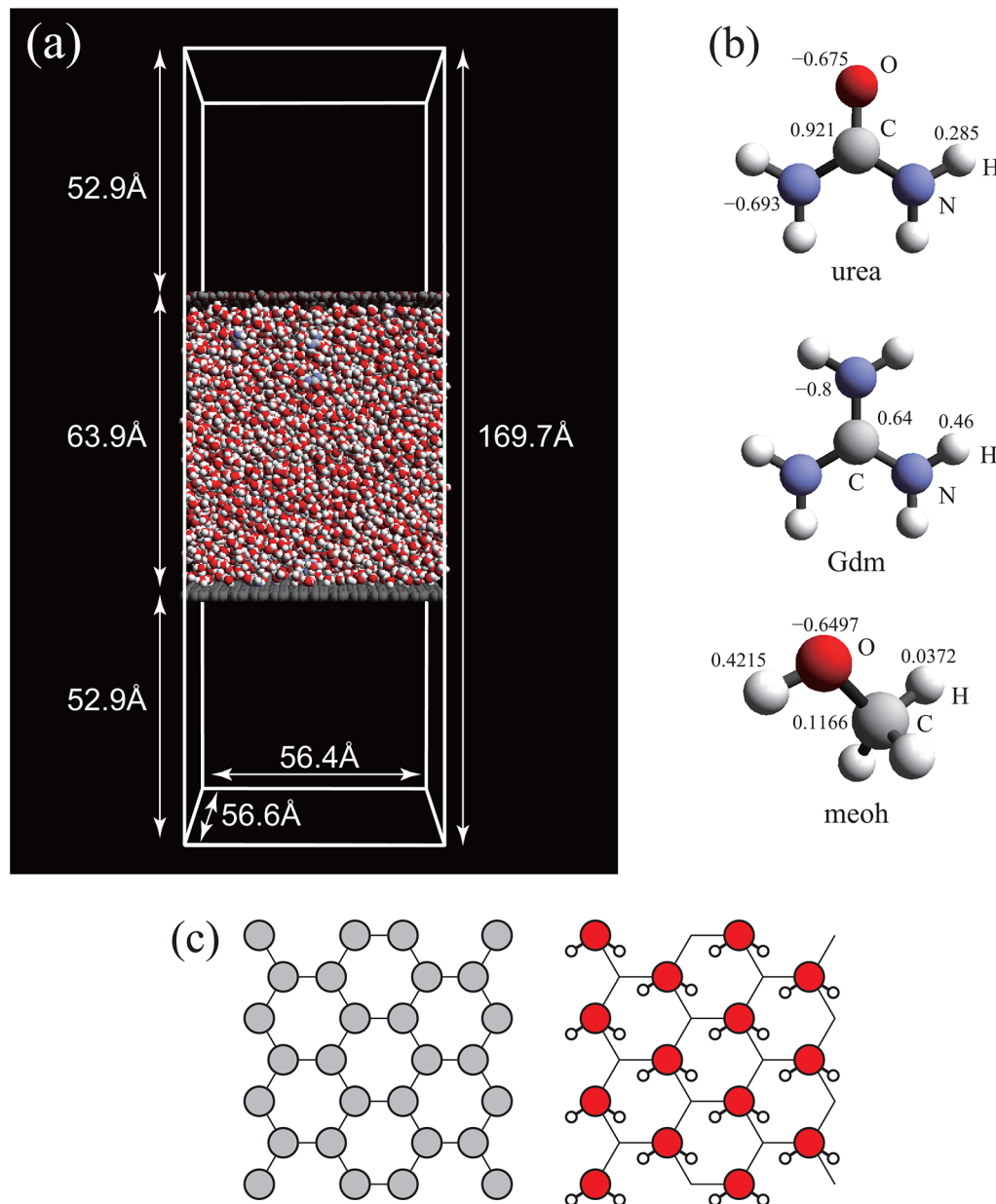


Figure 1. (a) A schematic plot of the simulation system. (b) Structures of denaturant molecules and atomic charges. (c) Layout of carbon atoms in the hydrophobic plate (left) and layout of fixed water molecules in the hydrophilic plate (right).

of urea in the two-stage denaturation process. In the first stage, urea molecules make favorable contacts with hydrophobic residues through the vdW interaction and then accumulate in the vicinity of the protein surface. Next, the urea molecules can penetrate into the interior of the protein, forming hydrogen bonds with the protein backbone and breaking the hydrophobic core. To confirm the effect of the vdW interaction on the hydrophobic core, Das and Zhou⁴ investigate behavior of urea molecules in an aqueous solution including a single-walled carbon nanotube. They found that urea molecules tend to occupy the interior region of the carbon nanotube due to the stronger dispersion interaction of urea with the carbon nanotube than with water.

Das and Mukhopadhyay⁹ reported that in the early stage of protein unfolding, urea molecules interact with the exposed polar groups of the protein via hydrogen bonding, and in the late stage, the well equilibrated unfolding state can be stabilized

by the dispersion interaction. However, Zhou et al.¹³ reported that they cannot reproduce Das and Mukhopadhyay's results, particularly the electrostatic interaction energy of bulk water. Canchi et al.¹⁷ found that the denaturation is driven by favorable direct interaction of urea with the protein through both electrostatic and vdW forces and quantified their contribution. Although determination of the dominant interaction for the protein denaturation has been controversial, many studies^{9–11,17} indicate two important functionalities of urea toward protein denaturation: hydrophobic interaction via the vdW force and hydrophilic interaction via the electrostatic force. A question then arises: which force is more dominant when both hydrophilic and hydrophobic species are present in water? The answer to this question would provide a better understanding of the urea-induced protein denaturation. In this simulation study, we design various confined fluid systems with hybrid confinement surfaces. Specifically, the slit nanopore

Table 1. Number of Molecules in Three Solution Systems^a

denat:water (%)	urea			GdmCl				meoh			
	N_{wat}	N_{denat}	$N_{\text{mol}} \text{ or } N_{\text{tot}}$	N_{wat}	N_{denat}	N_{Cl}	N_{mol}	N_{tot}	N_{wat}	N_{denat}	$N_{\text{mol}} \text{ or } N_{\text{tot}}$
1	5774	58	5832	5716	58	58	5774	5832	5774	58	5832
5	5540	292	5832	5276	278	278	5554	5832	5540	292	5832
10	5249	583	5832	4772	530	530	5302	5832	5249	583	5832
15	4957	875	5832	4310	761	761	5071	5832	4957	875	5832

^aFour ratios of denaturant molecules versus water molecules are considered for each system.

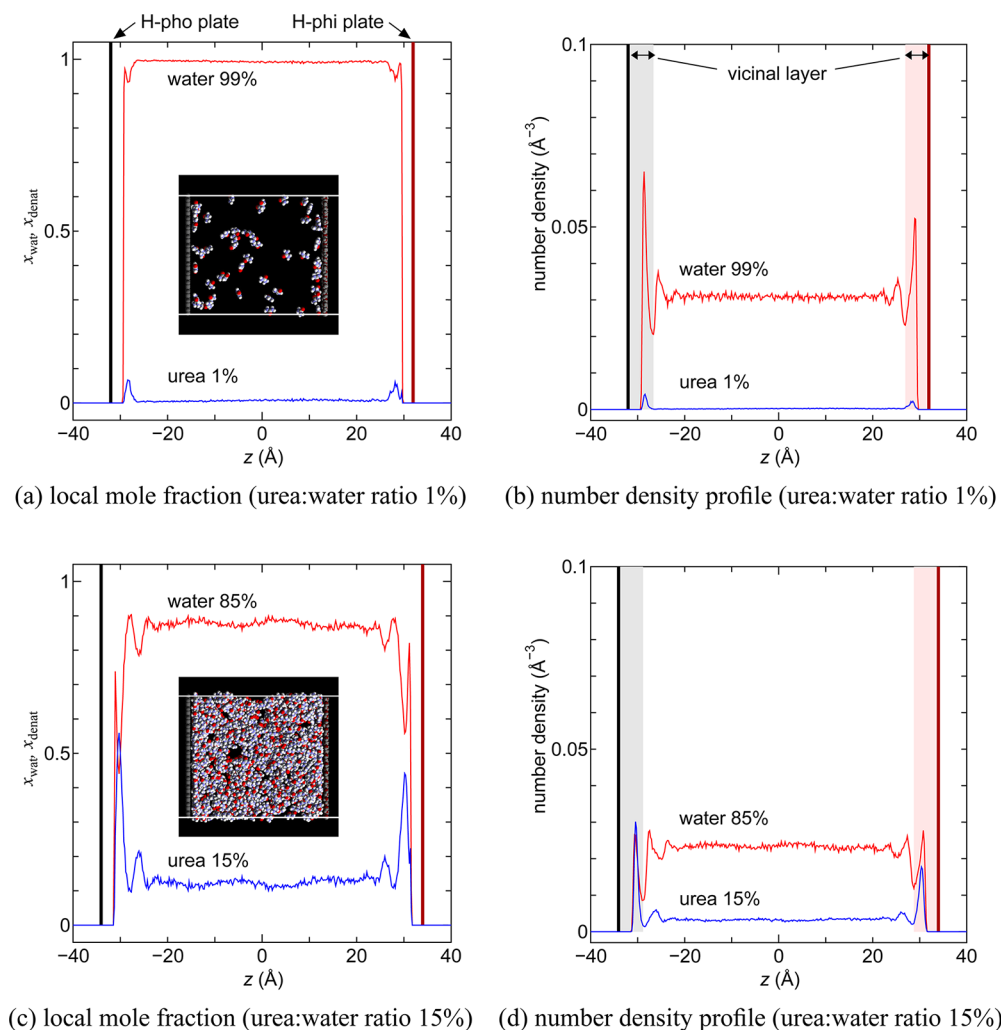


Figure 2. Local mole fraction and number density profiles, at urea/water ratios of 1% and 15%, respectively (results for 5% and 10% mole-fraction systems are in Figure S1).

consists of two opposing and parallel surfaces, one hydrophobic and another hydrophilic with an aqueous urea solution in between. Through molecular dynamics simulations, we monitor and record the preferential adsorption of denaturant molecules toward the two confinement surfaces. The population and lifetime of denaturant molecules in the vicinity of the confinement surfaces should provide additional quantitative measures of the preferential adsorption. A comparative study of preferential adsorption of denaturant molecules toward the two distinctly different surfaces would provide a way to evaluate the relative strength of vdW interaction and electrostatic interaction.

Besides urea, we also evaluate the relative denaturation capability of two other denaturant molecules, i.e., Gdm and methanol, through a comparative simulation study. It is known

that the denaturation effect of GdmCl is stronger than that of urea.²³ Slow dynamics of solvent in solutions with high concentrations of GdmCl has been reported.²⁰ Alcohols are also known as a denaturing agent. It has been reported that methanol can induce a structural change for certain proteins even though the proteins may exhibit extraordinary stability in urea and Gdm solutions.²⁶ In our simulations, both static and dynamic features of the three denaturants in the nanoslit are recorded, respectively. Our comparative studies suggest that urea, Gdm, and methanol may entail different denaturation mechanisms.

2. SIMULATION DETAILS

The simulation system is shown in Figure 1a. The hydrophobic and hydrophilic plates are fixed in parallel in the simulation cell,

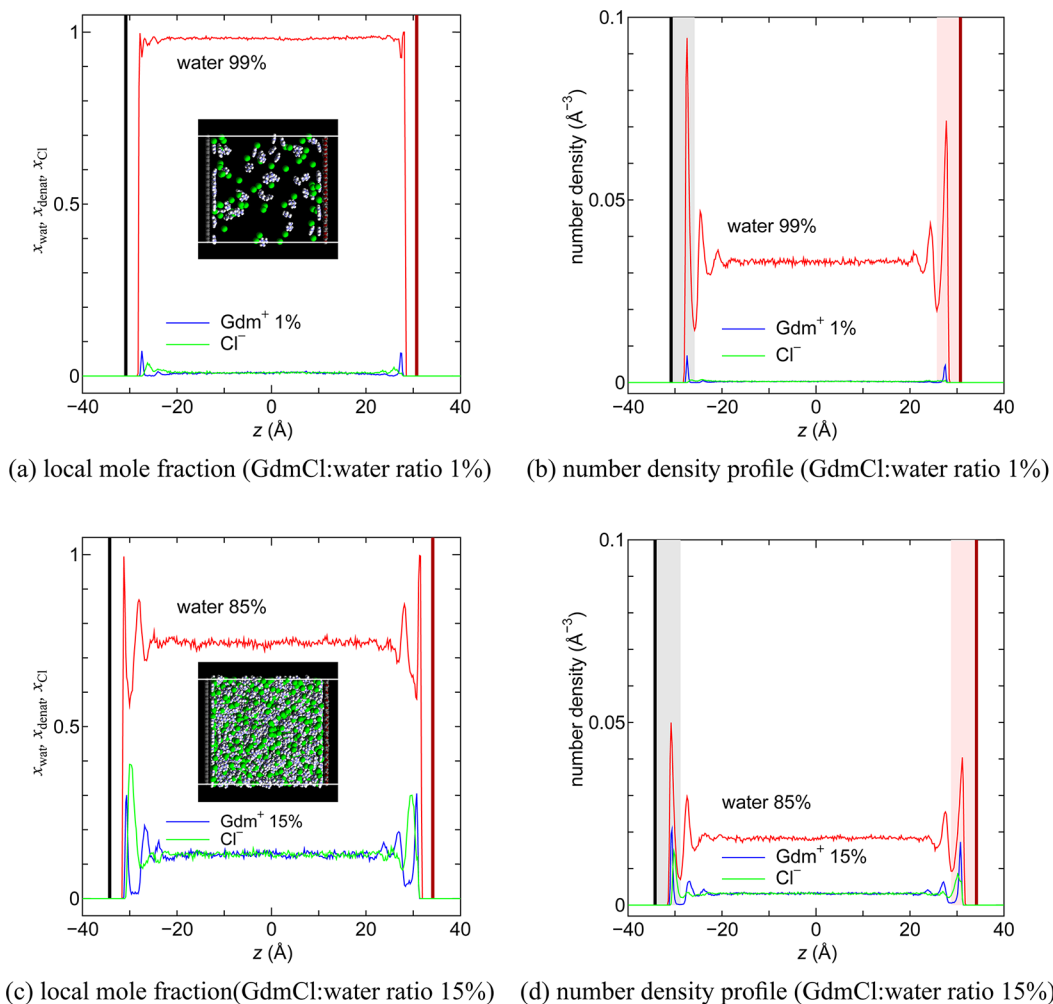


Figure 3. Local mole fraction and number density profiles of Gdm and Cl, at GdmCl/water ratios of 1% and 15%, respectively (results for 5% and 10% mole-fraction systems are in Figure S2).

and the aqueous solution of urea, Gdm, or methanol (Figure 1b) is confined between the two plates. The nanoslit system is separated by a vacuum in the normal (z) direction, as the periodic boundary conditions are applied in all three spatial directions. The hydrophobic plate is a graphene layer with hexagonally arranged carbon atoms (Figure 1c, left). During the simulation, carbon atoms are fixed. The lattice sites of the hydrophilic plate are the same as that of the graphene, but only the sites of one sublattice are occupied by water molecules (Figure 1c, right) due to the larger size of the water molecule. On the hydrophilic plate, each water molecule occupies a fixed position but is allowed to rotate freely.²⁷

The denaturant molecules, urea and Gdm, are treated as rigid molecules. The potential parameters for urea are given according to the Kirkwood–Buff (KBFF) theory.²⁸ This model has been frequently used for MD simulations.^{29–31} The parameter values of Gdm are based on the OPLS model.^{24,32} Methanol molecules are treated by a flexible model which includes bond, angle, and dihedral potentials whose parameters were developed by Caldwell and Kollman³³ and implemented in the Amber³⁴ force field. We use a rigid-body model of water, i.e., the SPC/E³⁵ model. The selection of the SPC/E and KBFF force fields for the water/urea solution is based on a recent benchmark test by Horinek and Netz,³⁶ who showed that the pair force fields give the best agreement with measured surface

tensions of water/urea solutions. In both SPC/E and KBFF force fields, the model potential of each atomic site includes typically two terms, a Coulomb term and a Lennard-Jones (LJ) term. Carbon atoms of the graphene are treated as LJ particles whose size and energy parameters are 3.4 Å and 0.2325 kJ/mol, respectively.³⁷

The time integration for the translational and rotational motion is undertaken using the velocity Verlet method and time-reversible algorithm.³⁸ The MD time step is set at 2.0 fs. In the system including methanol (flexible) molecules, the equations of motion are integrated using the multiple time step algorithm RESPA.³⁹ The time integration for the rotational motion of rigid molecules is also performed using a time-reversible algorithm.³⁸ We set the MD time step of the bond and angle integrations at 0.5 fs, that of the torsion integrations at 1.0 fs, and that of the nonbonding integrations at 2.0 fs. The long-range charge–charge interaction is calculated using the Ewald method. Before the sampling runs for the nanoslit system, bulk solutions are equilibrated for 400 ps. The simulation time of the sampling run is 5.0 ns.

For the denaturant solutions in the MD simulations, four ratios of the number of denaturant molecules to molecular water are considered, i.e., 1, 5, 10, and 15%. The numbers of molecules and ions are listed in Table 1. In this table, N_{wat} is the number of water molecules, N_{denat} is the number of denaturants

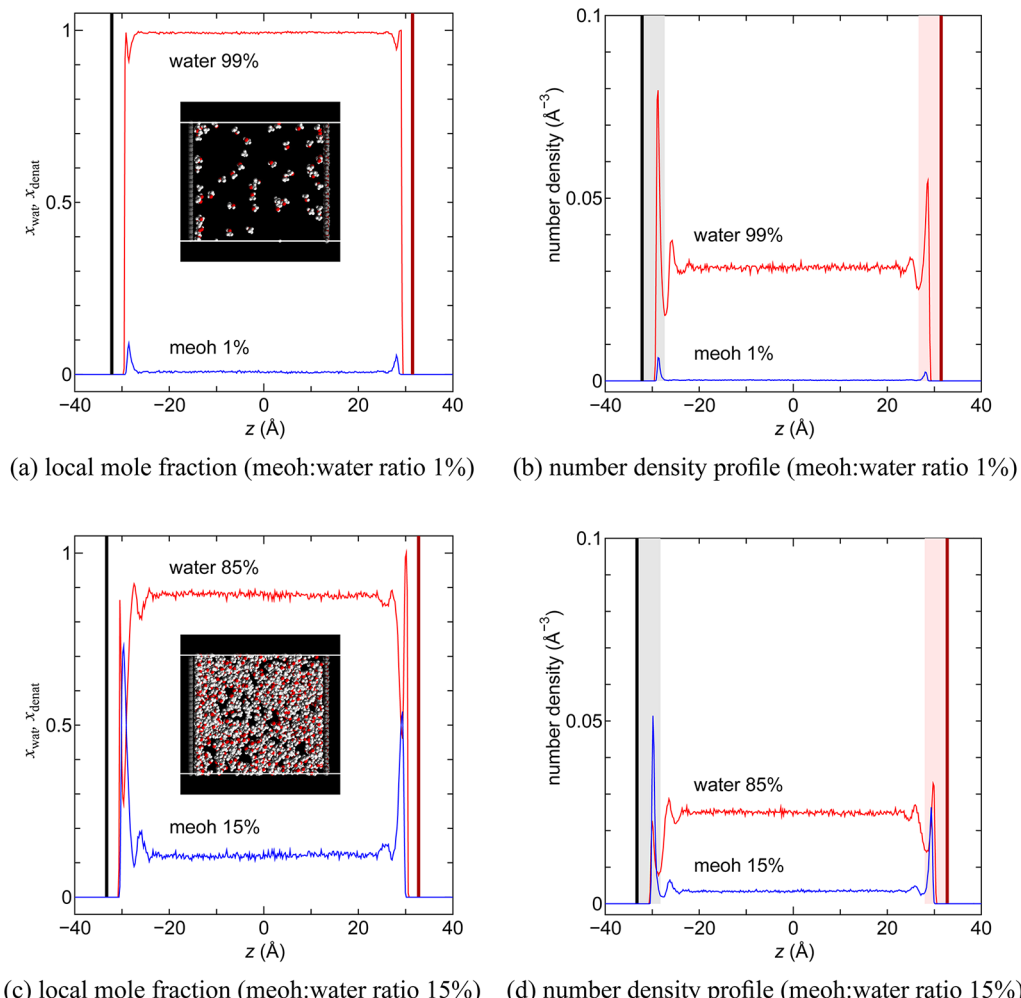


Figure 4. Local mole fraction and number density profiles of methanol (meoh), at meoh/water ratios of 1% and 15%, respectively (results for 5% and 10% mole-fraction systems are in Figure S3).

(urea, Gdm, and methanol), N_{Cl} is the number of Cl ions in the GdmCl system, N_{mol} is a sum of solvent and denaturant molecules, and N_{tot} is the total number of solvent and solute (denaturant and anion for GdmCl) molecules. Since Gdm and Cl are treated separately in our MD simulation, N_{mol} is not equivalent to N_{tot} in the GdmCl system. We can define the mole fraction of water, X_{wat} , and the denaturants, X_{denat} , respectively as

$$X_{\text{wat}} = \frac{N_{\text{wat}}}{N_{\text{mol}}}, X_{\text{denat}} = \frac{N_{\text{denat}}}{N_{\text{mol}}} \quad (1)$$

Note that X_{denat} is essentially the concentration of aqueous denaturant solutions. We also define the number of water and denaturant molecules in a local area, whose volume is $L_x \times L_y \times \Delta z$ (L_x and L_y are cell lengths of the x and y direction, $\Delta z = 0.2 \text{ \AA}$), as n_{wat} and n_{denat} , respectively, and their mole fractions as

$$x_{\text{wat}} = \frac{n_{\text{wat}}}{n_{\text{mol}}}, x_{\text{denat}} = \frac{n_{\text{denat}}}{n_{\text{mol}}} \quad (2)$$

where n_{mol} is a sum of solvent and solute molecules in the same area. These values will be discussed in the next section.

We use a special purpose computer, MDGRAPE-3, developed by Taiji et al.^{40–42} in RIKEN. The peak performance of an MDGRAPE-3 board with 12 MDGRAPE-3 chips (250 MHz)

is 2.16 Tflops. We use two special-purpose computers for the MD simulations: one for computing the real part of the Ewald sum and the other for computing the reciprocal-space part of the Ewald sum. All of the MD simulations are performed in the canonical ensemble. The temperature is controlled via velocity rescaling.⁴³

3. RESULTS AND DISCUSSIONS

3.1. Preferential Adsorption on Surfaces of Nanoslit.

Computed local mole fraction and number density profiles as a function of z -coordination for the confined urea, GdmCl, and methanol solutions are shown in Figures 2–4, respectively. Insets in the figures are snapshots of the system near the late stage, where water molecules are omitted for clarity. (Movies are provided in the Supporting Information (SI) as Movies S1, S2, and S3 for urea, GdmCl, and methanol in the 1% systems, respectively.) The locations of the hydrophobic and hydrophilic plates are illustrated by a vertical thick line and denoted as “H-pho plate” and “H-phi plate,” respectively. In the figures with number density profiles, the color-shaded areas highlight the first contact layer (vicinal layer) of the solution to either the hydrophobic or the hydrophilic plate. Here, the color-shaded section ends at the first minimum of the water density profile. The sharp high peaks of the water density profile near both plates demonstrate clearly the formation of the contact water

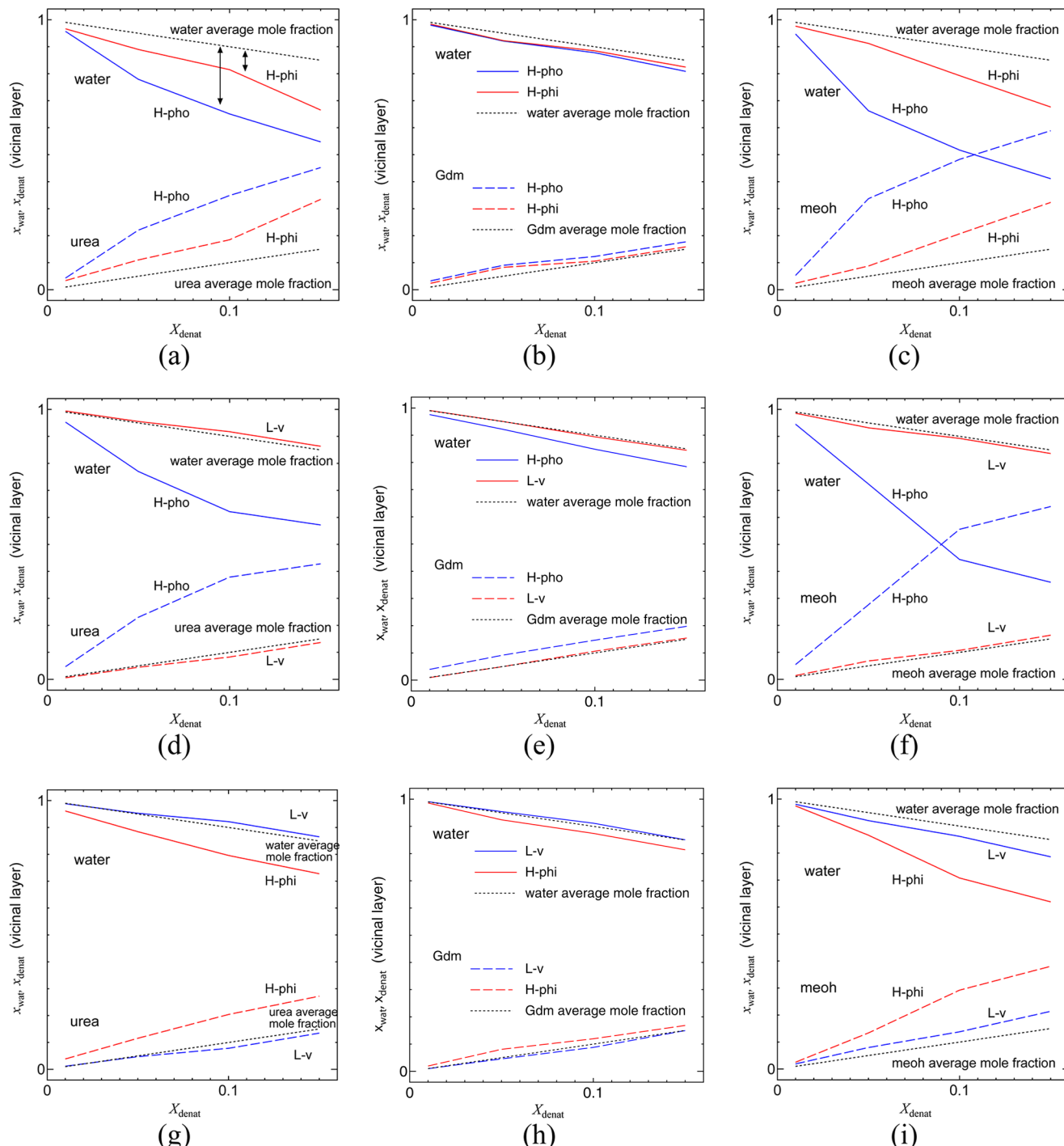


Figure 5. Local mole fraction of water and denaturant molecules in the vicinal layer of the hydrophobic (H-pho) plate, hydrophilic (H-phi) plate, or liquid–vapor (L-v) surface versus average mole fraction. The combinations of the denaturants, lower surface, and upper surface are (a) urea, H-pho, H-phi; (b) Gdm, H-pho, H-phi; (c) methanol (meoh), H-pho, H-phi; (d) urea, H-pho, L-v; (e) Gdm, H-pho, L-v; (f) meoh, H-pho, L-v; (g) urea, L-v, H-phi; (h) Gdm, L-v, H-phi; and (i) meoh, L-v, H-phi.

layer. Sharp peaks in the plot of the local mole fraction of water are also seen within the contact-layer region. This is because water molecules tend to be closer to the plates than the denaturant molecules due to smaller size of water molecules. Hereafter, we will neglect these peaks as they have little physical importance. On the other hand, it is of physical importance that the local mole fraction of denaturant molecules in the vicinal layer be higher than the average mole fraction of denaturant in the whole system. This result together with the

snapshot of denaturants clearly shows that the denaturant molecules tend to be near both plates.

In Figure 5, we plot the local mole fraction of denaturant molecules in the vicinal layer, whose volume is $L_x \times L_y \times \Delta z'$ ($\Delta z'$: vicinal layer width), versus the average mole fraction (dotted lines) in the nanoslit systems. As pointed out above, the vicinal mole fraction of urea, Gdm, and methanol is higher than the average mole fraction, indicating that all three denaturants are preferentially adsorbed on both the hydrophilic

and hydrophobic plates. As such, the vicinal mole fraction of water is expected to be smaller than the average mole fraction. The increase of the vicinal mole fraction of the denaturants and the decrease of the vicinal mole fraction of the water are symmetrical with respect to the middle horizontal line in Figure 5a and c. The average of the vicinal mole fraction of Gdm and Cl is symmetrical with that of the water in Figure 5b. Therefore, the vicinal mole fraction of water for each solution is suitable for a comparative study of preferential adsorption to the identical plates. Since the slope of the average mole fraction of water is -1 in Figure 5, the slope of the vicinal mole fraction of water must be less than -1 due to the preferential adsorption of denaturant molecules to the plates. As such, we define a relative preference factor, P_α (α = urea, Gdm, or methanol), as the absolute value of the local slope for the water curves shown in Figure 5:

$$P_\alpha = \left| \frac{dx_{\text{wat}}(c)}{dc} \right| \quad (3)$$

where $x_{\text{wat}}(c)$ is a linear fitting of the vicinal mole fraction curve and c is the average mole fraction of water. The difference between the average mole fraction and the vicinal mole fraction is indicated by arrows in Figure 5a.

3.2. Preferential Adsorption on Water-Vapor Interface. We also perform simulations in the nanoslit system where one of the plates is replaced by a water-vapor interface. It is known that the water-vapor interface can be viewed as a strongly hydrophobic surface. Typically, on a rough hydrophobic surface, the contact angle of a water droplet in the Cassie state⁴⁴ is greater than that in the Wenzel state.⁴⁵ This is because the water droplet in the Cassie state is in direct contact with only tips of the rough surface with air pockets being trapped between grooves of the rough structure, while in the Wenzel state the water droplet is in full contact with the entire surface. The relative preference factor P_α for the water-vapor interface is also computed. For the comparative studies, we consider three interfacial conditions: (i) hydrophobic and hydrophilic plates, (ii) hydrophobic plate and water-vapor interface, and (iii) water-vapor interface and hydrophilic plate. The relative preference factors are summarized in Figure 6.

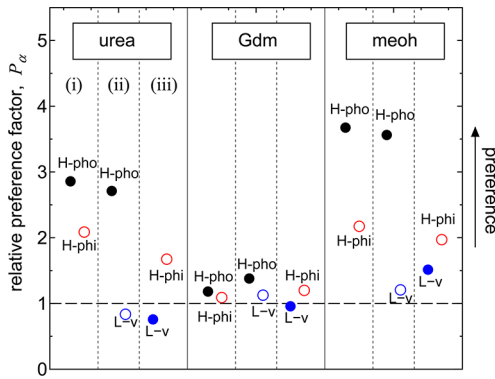


Figure 6. Computed relative preference factor for urea, Gdm, and methanol in three nanoslit systems with (i) hydrophobic and hydrophilic plates, (ii) hydrophobic plate and water-vapor interface, and (iii) water-vapor interface and hydrophilic plate.

In the urea solution, P_α for the hydrophobic plate (slope of blue lines in Figure 5a) is larger than that for the hydrophilic plate (slope of red lines). Both factors are greater than 1, while P_α for

the water-vapor interface is close to 1 (Figure 8). These results indicate that urea molecules are preferentially adsorbed to the rigid hydrophobic and hydrophilic plates, the hydrophobic plate in particular. The preferential adsorption of urea to the water-vapor interface is very modest, as the vicinal mole fraction is almost the same as the average mole fraction (Figure 8). Hence, even if both the hydrophobic plate and the water-vapor interface are hydrophobic, urea molecules tend to be preferably near the hydrophobic plate rather than the water-vapor interface. This difference in adsorption is likely due to the vdW interaction between the hydrophobic plate and the urea molecules, or the lack of vdW interaction for the vacuum (or vapor). For the GdmCl solution, all P_α values are close to 1, indicating that the preferential adsorption to both hydrophobic and hydrophilic plates is fairly weak (Figure 3c), and so is to the water-vapor interface. On the other hand, for the methanol solution, the P_α value for the hydrophobic plate is the largest (>3.5) among the three denaturants, indicating that methanol molecules are strongly preferred to be adsorbed to the rigid hydrophobic plate. In addition, the preferential adsorption to the hydrophilic plate is also appreciable for methanol molecules. If this bipreferentiality for both the hydrophobic and hydrophilic plates was required for strong denaturant, the denaturation effect of methanol would be large. However, it is known that urea and Gdm are stronger denaturants for most proteins. To resolve this issue, we suggest an alternative way to evaluate the effect of denaturation (see section 3.4).

3.3. Cross-Examination of the Preferential Adsorption

Based on Computed Surface Excess. In addition to the relative preference factor defined in eq 3, we have also computed the surface excess, $\Gamma_{\text{denat}} = \Gamma_i$ (i = urea, Gdm, or meoh), of the denaturants as it measures the extra amount of the denaturants per unit area at the Gibbs dividing surface of water. First, we compute the location of the Gibbs dividing surface based on the equation:

$$\Gamma_i = \int_{z_0}^{z_{\text{GDS}}} \rho_i(z) dz + \int_{z_{\text{GDS}}}^{z_1} \{\rho_i(z) - \rho_i^0\} dz \quad (4)$$

where z_0 is the position of the plate or the bottom of the simulation cell for the plate surface or the liquid–vapor surface, depending on the interface, z_1 is the center of the simulation cell, z_{GDS} is the Gibbs dividing surface where the surface excess of water is zero, $\rho(z)$ is the number density profile, and ρ_i^0 is the average number density at the center of solutions ($-20.0 \text{ \AA} < z < 20.0 \text{ \AA}$). The surface excess Γ_i is related to the surface tension, γ , through the Gibbs equation. It can be rewritten for a dilute solution as^{36,46}

$$\frac{d\gamma}{dX_{\text{denat}}} = -k_B T \frac{\Gamma_{\text{denat}}}{X_{\text{denat}}} \quad (5)$$

This equation shows that the mole-fraction dependence of the surface tension can be calculated from the surface excess normalized by the mole fraction.

We expect that the surface excess should be closely related to the relative preference factor as the former describes the extra amount of the denaturants per unit area at the Gibbs dividing surface, whereas the latter describes the preferential adsorption of denaturant in the vicinal layer over the bulk solution. To gain more insight into this correlation, we compute the surface excess as shown in Figure 7a,b,c. The normalized surface excesses are summarized in Figure 7d, to be compared with the relative preference factor in Figure 6. All values in Figure 7 are

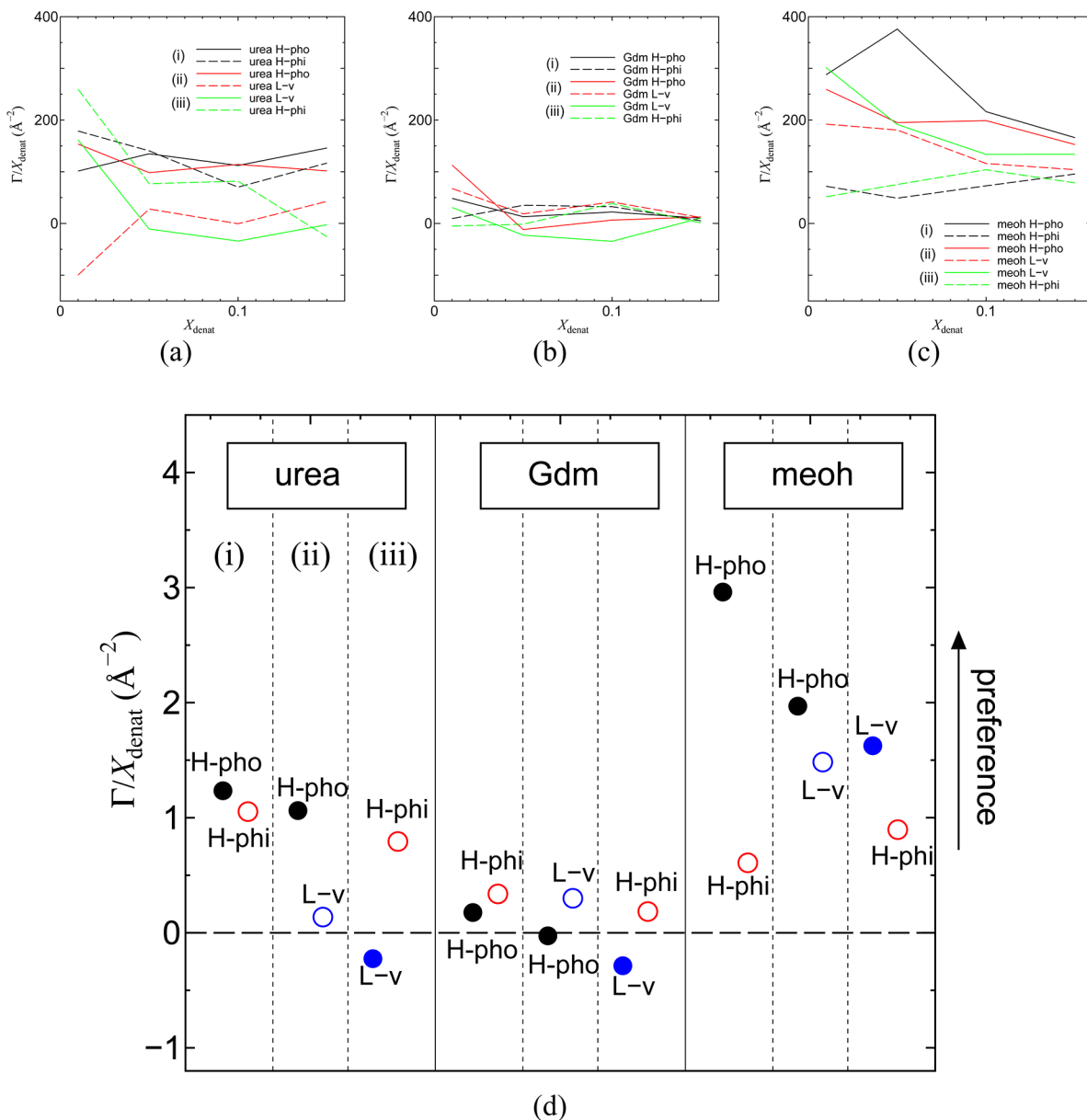


Figure 7. The surface excess (at the Gibbs dividing surface of water) normalized by the mole fraction of denaturants. (a) The mole fraction dependence of urea, (b) Gdm, and (c) methanol. (d) A summary of the normalized surface excess at difference interfaces. The plotted values are based on the average of 0.05 and 0.10 mol-fraction systems.

based on the average for the 0.05 and 0.10 mol-fraction systems. The normalized surface excess for the 0.01 mol-fraction system is omitted due to the large fluctuation. The normalized surface excess for the 0.15 mol-fraction system is also omitted because eq 5 is applicable only for dilute solutions. We find that in most cases the trend of preferential adsorption described by the normalized surface excess is in good agreement with that described by the preference factor. The only exception is the strong preferential adsorption of methanol to the water-vapor interface as predicted from the normalized surface excess. This result is consistent with that concluded from a previous simulation study.⁴⁶ Such a strong adsorption of methanol to the water-vapor interface renders the vicinal layer much wider than the width of the vicinal layer to the hydrophilic plate (see Figure S5), hence the smaller preference factor for the methanol at the water-vapor interface than that for the methanol near the hydrophilic plate (see Figure 2).

3.4. Dynamic Properties of Denaturant near Surfaces of Nanoslit. Here, the dynamic properties of denaturant are assessed based on the relaxation (or resident) time τ for the denaturant molecules in the vicinal layer. Here, τ is evaluated by the single-exponential fitting of the correlation function (with t_0 being defined as the origin of time):

$$C(t) = \frac{\langle \sum_i s_i(t_0) s_i(t) \rangle}{\langle \sum_i s_i(t_0) s_i(t_0) \rangle} \quad (6)$$

where

$$s_i(t) = \begin{cases} 1 & (\text{in the vicinal layer}) \\ 0 & (\text{otherwise}) \end{cases} \quad (7)$$

Note that when the mole fraction of denaturants is very small, the fluctuation of the fitting results can be quite large as the

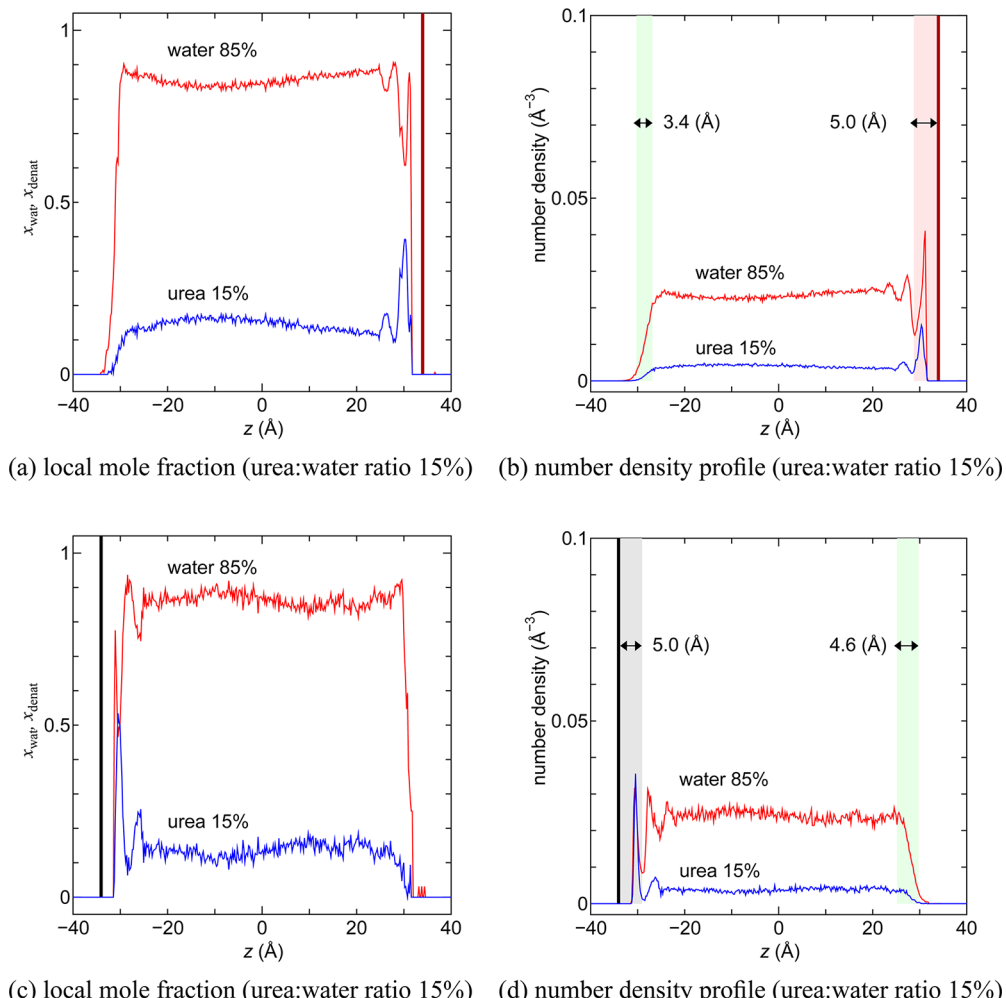


Figure 8. Local mole fraction and number density profiles of urea at a urea/water ratio of 5% in the nanoslit system with (a and b) the water-vapor interface and the hydrophilic plate and (c and d) the hydrophobic plate and the water-vapor interface. (The same figures but for Gdm and meoh solutions are shown in Figures S4 and S5, respectively.)

number of denaturant molecules in the vicinal layer would be very small as well. Thus, we mainly focus on the correlation function for the highest mole fraction (0.15) considered in this study to compute the relaxation time. The results of τ are listed in Table 2, which show that typically $\tau^{\text{Gdm}} \gg \tau^{\text{urea}} > \tau^{\text{meoh}}$. It is

Table 2. Computed Relaxation Time of Denaturant Molecules in the Vicinal Layers

		relaxation time τ (ns)					
condition		urea		Gdm		meoh	
H-pho	H-phi	1.70	0.57	26.6	4.54	0.39	0.13
H-pho	L-v	1.60	0.39	43.0	0.91	0.34	0.15
L-v	H-phi	0.35	1.00	1.03	7.34	0.12	0.13

remarkable that the residence time of Gdm in the vicinal layer of the hydrophobic plate is 1 or 2 orders of magnitude longer than that of urea or methanol. Even though Gdm does not show a high tendency of preferential adsorption to the hydrophobic plate compared to urea and methanol, once it is adsorbed onto the plate, Gdm can bind more strongly to the hydrophobic plate due to the stronger vdW interaction than urea or methanol. Note also that the relatively slow dynamics of Gdm were reported in a previous study.²⁰ Because the Gdm

molecules in the vicinal layer effectively make a pseudocharged surface, the Cl^- ions are also attracted to the hydrophobic plate as well. Together, both charged species form an electric double layer.⁴⁷ As a result, the diffusivity of water molecules in the electric double layer becomes slower. Hence, the local liquid structure of water in the vicinal layer differs from that of bulk water, and the peak height of the number density profile is higher for the GdmCl system (see Figure 3b,d). This structural change in the vicinal layer might be relevant to the protein denaturation.

On the other hand, a much shorter residence time for methanol is observed in the vicinal layer. Although this is a kinetic effect, its close correlation with the weaker denaturing effect of methanol is interesting, even though methanol exhibits the highest tendency for preferential adsorption to the hydrophobic plate. Last, the residence time in the vicinal layer for urea is in between that of Gdm and methanol, and again, interestingly, this kinetic effect is correlated with that middle denaturing capability of urea among the three denaturants. For all three denaturants, their preference factor toward the hydrophobic plate is always larger than that toward the hydrophilic plate and water-vapor interface. Hence, the residence time in the vicinal layer of the hydrophobic plate is

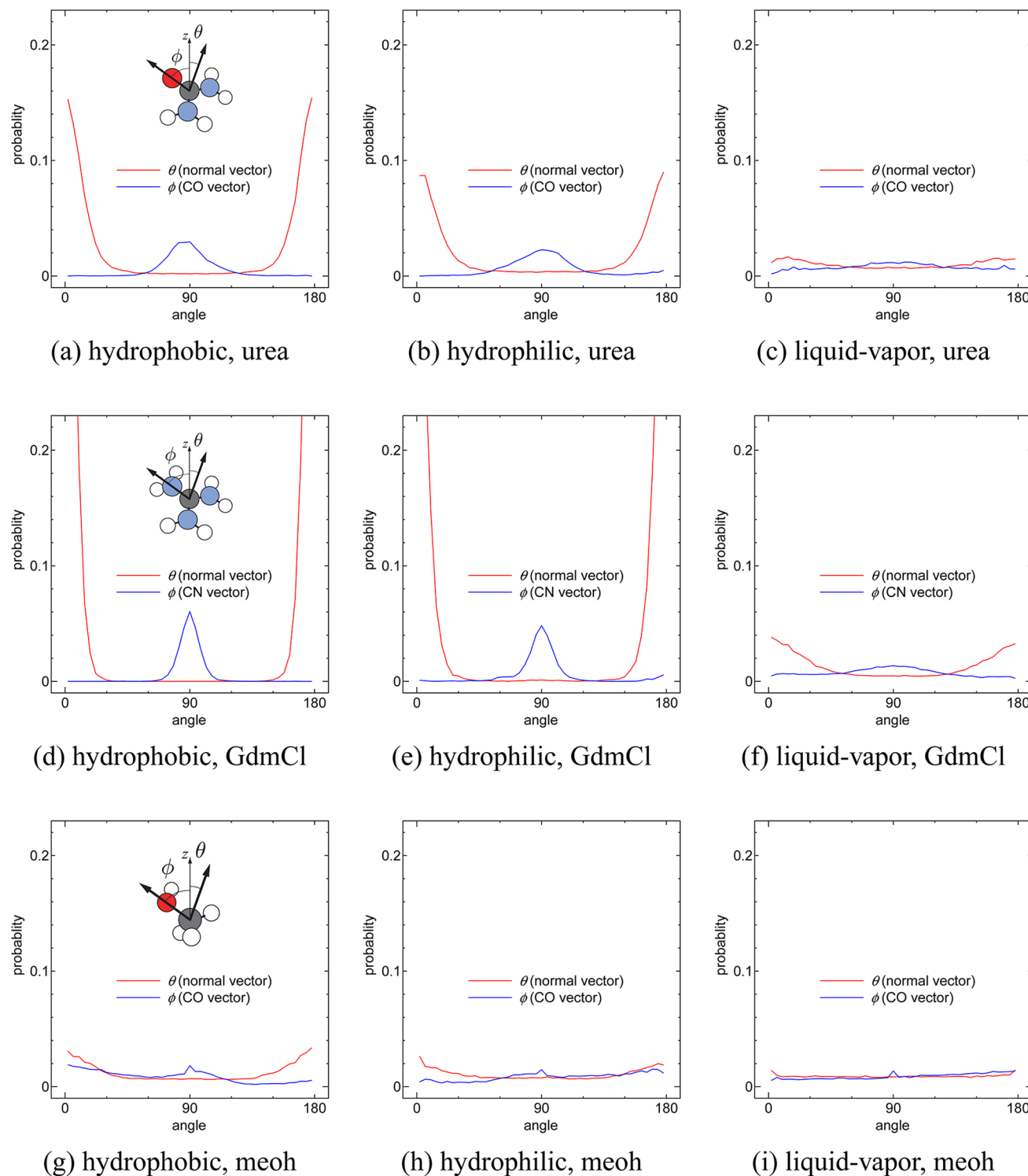


Figure 9. Angle distributions of urea, Gdm, and meoh in the vicinal layer near (a, d, and g) the hydrophobic plate, (b, e, and h) the hydrophilic plate, and (c, f, and i) the water-vapor interface (or vacuum surface).

always longer than that of the hydrophilic plate or than near the water-vapor interface (Table 2).

Finally, we compute the angle distribution of urea, Gdm, and methanol molecules in the vicinal layer of both plates and near the water-vapor interface. To this end, we define two vectors on each denaturant molecule: One is the vector connecting two distinctive atoms, specifically, the C–O vector for urea and methanol, and the C–N vector for Gdm. Another vector is

normal to the molecular plane for urea and Gdm or is normal to the C–O–H_O plane for methanol, where H_O is the hydrogen atom binding with O. To estimate the probability distribution, the angle between an arbitrary z-axis and the two vectors is defined as θ and ϕ , respectively (Figure 9 insets). The computed probabilities divided by sin θ or sin ϕ are shown in Figure 9. The angle distribution of urea and Gdm near the hydrophobic and hydrophilic plate exhibits a peak around 90°

for θ and two peaks around 0° and 180° for ϕ , respectively. These distributions suggest that planar molecules like urea and Gdm tend to be in parallel with the rigid plates. This tendency is greater near the hydrophobic plate than near the hydrophilic plate. The accumulation of urea and Gdm near the plates may induce stacking structures. Indeed, the stacking structures were observed in previous studies.^{17,21,23–25,48} Mason et al.²⁵ indicate that the efficiency as a denaturant is due to its ability to simultaneously interact favorably with both water and hydrophobic side chains of proteins. As such, the high tendency for urea or Gdm molecules being in parallel with both the hydrophobic and hydrophilic plates may be a manifestation of their strong denaturing efficiency. Since peaks in the angle distributions of urea and Gdm near the water-vapor interface are all relatively low, the tendency for urea or Gdm taking parallel orientation with respect to the water-vapor interface should be weak. On the other hand, the angle distribution of methanol molecules does not show any notable high peaks near either rigid plates or water-vapor interface as shown in Figure 9g,h,i. In fact, the orientation of methanol molecules appears to be randomly distributed in the vicinal layer of the hydrophobic and hydrophilic plates or near the water-vapor interface. This might be another reason that the denaturing efficiency of methanol is not as high as that of urea or Gdm.

4. CONCLUSION

We have performed a systematic comparative study of preferential adsorption and dynamical properties of three denaturant molecules near hydrophobic or hydrophilic plates or the water-vapor interface. Our results show that the relative preference factors to the hydrophobic and hydrophilic plates for all three denaturants are greater than 1.0 for the hydrophobic and hydrophilic plates, and those to the water-vapor interface are around 1.0. The occupancy of the denaturants in the vicinal layer of the hydrophobic and hydrophilic plates is larger than that of water molecules, indicating that the denaturants tend to approach both hydrophobic and hydrophilic plates. Near the water-vapor interface, the occupancy of the denaturant and water molecules are more or less the same. This feature of denaturant molecules is contrary to that of typical amphiphilic molecules (e.g., surfactants) which tend to accumulate on the water-vapor interface. The order of the relative preference factor in the vicinal layer of both plates is methanol > urea > Gdm. The relative preference factor to the hydrophobic plate is greater than that to the hydrophilic plate for all denaturants.

Our simulation also shows that the order of the residence time in the vicinal layer is Gdm \gg urea $>$ methanol. This order is in reverse to the order of the relative preference factor, suggesting that the three denaturants may entail different mechanisms of protein denaturation. Among the three denaturants, Gdm has the highest capability of the long-time binding with both hydrophobic and hydrophilic plates, while methanol has the highest capability of preferential adsorption to both plates. Urea possesses both capabilities in balance. In addition, our results of the angle distribution indicate that the planar molecules like urea and Gdm tend to be in parallel with the hydrophobic and hydrophilic plates when in the vicinal layer. This feature seems correlated with the feature of stacking aggregation near both plates, a signature of high denaturing efficiency. In view of their different capabilities and adsorption characteristics with hydrophobic and hydrophilic chemical

sections, one may choose a denaturant based on structural features of targeted proteins.

■ ASSOCIATED CONTENT

S Supporting Information

Movies for urea, GdmCl, and methanol with the hydrophobic and hydrophilic plates in the 1% systems; local mole fraction and number density profiles with the hydrophobic and the hydrophilic plate for urea, Gdm, and methanol in 5% and 10% systems; and local mole fraction and number density profiles including the liquid–vapor surface for Gdm and methanol systems. These materials are available free of charge via the Internet at <http://pubs.acs.org>.

■ AUTHOR INFORMATION

Corresponding Author

*E-mail: koishi@u-fukui.ac.jp, xzeng1@unl.edu.

Notes

The authors declare no competing financial interest.

■ ACKNOWLEDGMENTS

This research was supported by JSPS KAKENHI Grant Number 22740253. X.C.Z. is supported by U.S. NSF (grant no. CBET-1066947), ARL (grant no. W911NF1020099), and the Nebraska Research Initiative.

■ REFERENCES

- Ikeguchi, M.; Nakamura, S.; Shimizu, K. Molecular Dynamics Study on Hydrophobic Effects in Aqueous Urea Solutions. *J. Am. Chem. Soc.* **2001**, *123*, 677–682.
- Lee, M.-E.; van der Vegt, N. F. A. Does Urea Denature Hydrophobic Interactions? *J. Am. Chem. Soc.* **2006**, *128*, 4948–4949.
- Idrissi, A.; Gerard, M.; Damay, P.; Kiselev, M.; Puhovsky, Y.; Cinar, E.; Lagant, P.; Vergoten, G. The Effect of Urea on the Structure of Water: A Molecular Dynamics Simulation. *J. Phys. Chem. B* **2010**, *114*, 4731–4738.
- Das, P.; Zhou, R. Urea-Induced Drying of Carbon Nanotubes Suggests Existence of a Dry Globule-like Transient State During Chemical Denaturation of Proteins. *J. Phys. Chem. B* **2010**, *114*, 5427–5430.
- Tobi, D.; Elber, R.; Thirumalai, D. The dominant interaction between peptide and urea is electrostatic in nature: A molecular dynamics simulation study. *Biopolymers* **2003**, *68*, 359–369.
- Das, A.; Mukhopadhyay, C. Urea-Mediated Protein Denaturation: A Consensus View. *J. Phys. Chem. B* **2009**, *113*, 12816–12824.
- Klimov, D. K.; Straub, J. E.; Thirumalai, D. Aqueous urea solution destabilizes Ab16–22 oligomers. *Proc. Natl. Acad. Sci. U. S. A.* **2004**, *101*, 14760–14765.
- Berteotti, A.; Barducci, A.; Parrinello, M. Effect of Urea on the beta-Hairpin Conformational Ensemble and Protein Denaturation Mechanism. *J. Am. Chem. Soc.* **2011**, *133*, 17200–17206.
- Das, A.; Mukhopadhyay, C. Reply to the “Comment on ‘Urea-Mediated Protein Denaturation: A Consensus View’”. *J. Phys. Chem. B* **2011**, *115*, 1327–1328.
- Stumpe, M. C.; Grubmuller, H. Interaction of Urea with Amino Acids: Implications for Urea-Induced Protein Denaturation. *J. Am. Chem. Soc.* **2007**, *129*, 16126–16131.
- Hua, L.; Zhou, R.; Thirumalai, D.; Berne, B. J. Urea denaturation by stronger dispersion interactions with proteins than water implies a 2-stage unfolding. *Proc. Natl. Acad. Sci. U. S. A.* **2008**, *105*, 16928–16933.
- Zangi, R.; Zhou, R.; Berne, B. Urea’s Action on Hydrophobic Interactions. *J. Am. Chem. Soc.* **2009**, *131*, 1535–1541.
- Zhou, R.; Li, J.; Hua, L.; Yang, Z.; Berne, B. J. Comment on “Urea-Mediated Protein Denaturation: A Consensus View”. *J. Phys. Chem. B* **2011**, *115*, 1323–1326.

- (14) Li, W.; Zhou, R.; Mu, Y. Salting Effects on Protein Components in Aqueous NaCl and Urea Solutions: Toward Understanding of Urea-Induced Protein Denaturation. *J. Phys. Chem. B* **2012**, *116*, 1446–1451.
- (15) Caballero-Herrera, A.; Nordstrand, K.; Berndt, K. D.; Nilsson, L. Effect of Urea on Peptide Conformation in Water: Molecular Dynamics and Experimental Characterization. *Biophys. J.* **2005**, *89*, 842–857.
- (16) Wei, H.; Fan, Y.; Gao, Y. Q. Effects of Urea, Tetramethyl Urea, and Trimethylamine N-Oxide on Aqueous Solution Structure and Solvation of Protein Backbones: A Molecular Dynamics Simulation Study. *J. Phys. Chem. B* **2010**, *114*, 557–568.
- (17) Canchi, D. R.; Paschek, D.; Garcia, A. E. Equilibrium Study of Protein Denaturation by Urea. *J. Am. Chem. Soc.* **2010**, *132*, 2338–2344.
- (18) Vanzi, F.; Madan, B.; Sharp, K. Effect of the Protein Denaturants Urea and Guanidinium on Water Structure: Structural and Thermodynamic Study. *J. Am. Chem. Soc.* **1998**, *120*, 10748–10753.
- (19) O'Brien, E. P.; Dima, R. I.; Brooks, B.; Thirumalai, D. Interactions between Hydrophobic and Ionic Solutes in Aqueous Guanidinium Chloride and Urea Solutions: Lessons for Protein Denaturation Mechanism. *J. Am. Chem. Soc.* **2007**, *129*, 7346–7353.
- (20) Camilloni, C.; Rocco, A. G.; Eberini, I.; Gianazza, E.; Broglia, R. A.; Tiana, G. Urea and Guanidinium Chloride Denature Protein L in Different Ways in Molecular Dynamics Simulations. *Biophys. J.* **2008**, *94*, 4654–4661.
- (21) Mehrnejad, F.; Khadem-Maaref, M.; Ghahremanpour, M.; Doustdar, F. Mechanisms of amphipathic helical peptide denaturation by guanidinium chloride and urea: a molecular dynamics simulation study. *J. Comput.-Aided Mol. Des.* **2010**, *24*, 829–841.
- (22) Heyda, J.; Kozisek, M.; Bednarova, L.; Thompson, G.; Konvalinka, J.; Vondrasek, J.; Jungwirth, P. Urea and Guanidinium Induced Denaturation of a Trp-Cage Miniprotein. *J. Phys. Chem. B* **2011**, *115*, 8910–8924.
- (23) Li, W.; Mu, Y. Dissociation of hydrophobic and charged nano particles in aqueous guanidinium chloride and urea solutions: A molecular dynamics study. *Nanoscale* **2012**, *4*, 1154–1159.
- (24) Godawat, R.; Jamadagni, S. N.; Garde, S. Unfolding of Hydrophobic Polymers in Guanidinium Chloride Solutions. *J. Phys. Chem. B* **2010**, *114*, 2246–2254.
- (25) Mason, P. E.; Neilson, G. W.; Enderby, J. E.; Saboungi, M.-L.; Dempsey, C. E.; MacKerell, A. D.; Brady, J. W. The Structure of Aqueous Guanidinium Chloride Solutions. *J. Am. Chem. Soc.* **2004**, *126*, 11462–11470.
- (26) Sundd, M.; Kundu, S.; Jagannadham, M. V. Alcohol-Induced Conformational Transitions in Ervatamin C. An a-Helix to b-Sheet Switcheroo. *J. Prot. Chem.* **2000**, *19*, 169–176.
- (27) Koishi, T.; Yoo, S.; Yasuoka, K.; Zeng, X. C.; Narumi, T.; Susukita, R.; Kawai, A.; Furusawa, H.; Suenaga, A.; Okimoto, N.; Futatsugi, N.; Ebisuzaki, T. Nanoscale Hydrophobic Interaction and Nanobubble Nucleation. *Phys. Rev. Lett.* **2004**, *93*, 185701.
- (28) Weerasinghe, S.; Smith, P. E. A Kirkwood-Buff derived force field for mixtures of urea and water. *J. Phys. Chem. B* **2003**, *107*, 3891–3898.
- (29) Mountain, R. D.; Thirumalai, D. Importance of Excluded Volume on the Solvation of Urea in Water. *J. Phys. Chem. B* **2004**, *108*, 6826–6831.
- (30) Kokubo, H.; Pettitt, B. M. Preferential Solvation in Urea Solutions at Different Concentrations: Properties from Simulation Studies. *J. Phys. Chem. B* **2007**, *111*, 5233–5242.
- (31) Koishi, T.; Yasuoka, K.; Zeng, X. C.; Fujikawa, S. Molecular dynamics simulations of urea–water binary droplets on flat and pillared hydrophobic surfaces. *Faraday Discuss.* **2010**, *146*, 185–193.
- (32) Jorgensen, W. L.; Tirado-Rives, J. The OPLS [optimized potentials for liquid simulations] potential functions for proteins, energy minimizations for crystals of cyclic peptides and crambin. *J. Am. Chem. Soc.* **1988**, *110*, 1657–1666.
- (33) Caldwell, J. W.; Kollman, P. A. Structure and Properties of Neat Liquids Using Nonadditive Molecular Dynamics: Water, Methanol, and N-Methylacetamide. *J. Phys. Chem.* **1995**, *99*, 6208–6219.
- (34) Case, D. A.; Cheatham, T. E.; Darden, T.; Gohlke, H.; Luo, R.; Merz, K. M.; Onufriev, A.; Simmerling, C.; Wang, B.; Woods, R. J. The Amber biomolecular simulation programs. *J. Comput. Chem.* **2005**, *26*, 1668–1688.
- (35) Berendsen, H. J. C.; Grigera, J. R.; Straatsma, T. P. The missing term in effective pair potentials. *J. Phys. Chem.* **1987**, *91*, 6269–6271.
- (36) Horinek, D.; Netz, R. R. Can Simulations Quantitatively Predict Peptide Transfer Free Energies to Urea Solutions? Thermodynamic Concepts and Force Field Limitations. *J. Phys. Chem. A* **2011**, *115*, 6125–6136.
- (37) Bhethanabotla, V. R.; Steele, W. A. Molecular dynamics simulations of oxygen monolayers on graphite. *Langmuir* **1987**, *3*, 581–587.
- (38) Matubayasi, N.; Nakahara, M. Reversible molecular dynamics for rigid bodies and hybrid Monte Carlo. *J. Chem. Phys.* **1999**, *110*, 3291–3301.
- (39) Tuckerman, M.; Berne, B. J.; Martyna, G. J. Berne Reversible multiple time scale molecular dynamics. *J. Chem. Phys.* **1992**, *97*, 1990–2001.
- (40) Taiji, M.; Narumi, T.; Ohno, Y.; Futatsugi, N.; Suenaga, A.; Takada, N.; Konagaya, A. Protein explorer: A peta flops special-purpose computer system for molecular dynamics simulations. *Proceedings of the SC2003 (High Performance Networking and Computing)*; Phoenix, AZ, Nov 15–21, 2003.
- (41) Taiji, M. MDGRAPE-3 chip: A 165-Gflops application-specific LSI for molecular dynamics simulations. *Proceedings of the HOT CHIPS 16 (A Symposium on High Performance Chips)*; Stanford, CA, Aug 22–24, 2004.
- (42) Narumi, T.; Ohno, Y.; Okimoto, N.; Koishi, T.; Suenaga, A.; Futatsugi, N.; Yanai, R.; Himeno, R.; Fujikawa, S.; Ikei, M.; Taiji, M. A 55 TFLOPS simulation of amyloid-forming peptides from yeast prion Sup35 with the special-purpose computer system MDGRAPE-3. *Proceedings of the SC06 (High Performance Computing, Networking, Storage and Analysis)*; Tampa, FL, Nov 11–17, 2006.
- (43) Allen, M. P.; Tildesley, D. J. *Computer Simulation of Liquids*; Oxford Science: Oxford, U. K., 1987.
- (44) Cassie, A. B. D.; Baxter, S. Wettability of porous surfaces. *Trans. Faraday Soc.* **1944**, *40*, 546–551.
- (45) Wenzel, R. N. Resistance of solid surfaces to wetting by water. *Ind. Eng. Chem.* **1936**, *28*, 988–994.
- (46) Matsumoto, M.; Takaoka, Y.; Kataoka, Y. Liquid-vapor interface of water-methanol mixture. I. Computer simulation. *J. Chem. Phys.* **1993**, *98*, 1464–1472.
- (47) Israelachvili, J. N. *Intermolecular and Surface Forces*; Academic Press: London, 1992.
- (48) Lim, W. K.; Rosgen, J.; Englander, S. W. Urea, but not guanidinium, destabilizes proteins by forming hydrogen bonds to the peptide group. *Proc. Natl. Acad. Sci. U. S. A.* **2009**, *106*, 2595–2600.